

2.3 kV – A new voltage class for Si IGBT and Si FWD

Frank Umbach¹, Philip Brandt¹, Sergio Mansueto¹, Wilhelm Rusche¹, Andreas Korzenietz¹, Damiano Cassese², Ute Queitsch³

¹ Infineon Technologies AG, Germany

² Infineon Technologies Austria AG, Austria

³ Infineon Technologies Dresden GmbH & Co. KG, Germany

Corresponding author: Frank Umbach, Frank.Umbach@infineon.com

The Power Point Presentation will be available after the conference.

Abstract

In this paper new silicon IGBT and diode technologies of a new voltage class are presented. These technologies are being developed to meet the requirements of solar central converters with a DC-link voltage of 1500 V. Especially the cosmic radiation failure rate is limiting the usage of devices with nominal voltages up to $V_{\text{NOM}}=1700$ V. The new IGBT is based on Infineon's most recent TRENCHSTOP™ IGBT7 technology, and adapted to the needs of the solar application. The new diode is based on Infineon's most recent emitter-controlled 7th generation technology and optimized for the usage as freewheeling diode for the 2.3 kV IGBT. The cosmic radiation robustness of both devices is designed for applied DC-link voltages up to 1500 V. The performance of the devices is designed to be operated either in standard 2-level topology or in a 3-level NPC2 topology when used in combination with a 1200 V module in common collector configuration.

1 Introduction

In the application of central inverters for huge megawatt (MW) solar plants, there is a clear trend towards a DC-link voltage of 1500 V. Currently a DC-link voltage of 1500 V is generally implemented by a series connection of 1200 V devices, for example in a NPC1 topology. The usage of 1700 V devices is limited by the cosmic radiation failure rate of this voltage class. To enable the usage of 1500 V DC-link voltage with a standard half-bridge configuration or in a NPC2 topology, a new voltage class has been introduced to overcome the well-known challenges in building an NPC1 topology with discrete power modules.

Consequently, the new voltage class is determined by the cosmic radiation requirements. To allow applied voltages of up to 1500 V at low failure rates, a certain vertical design of the chips is required. Several combinations of device thickness and base material doping were evaluated in irradiation experiments, and a design suitable for DC-link voltages up to 1500 V was chosen.

The selection of a cell concept and first characterization results are described as well as measurements of a half-bridge module built in the

PrimePACK™ 3+ package. Finally, an estimation of the reachable output power of the module in standard half-bridge 2-level topology as well as in 3-level NPC2 topology is provided. For a detailed description of the NPC2 topology, see [4].

2 Determination of $V_{\text{NOM}} = 2.3$ kV

Figure 1 shows the cosmic radiation failure rate of the 2.3 kV IGBT as a function of the applied voltage for different variants with regard to the vertical design of the devices. The same evaluation has been done for the 2.3 kV diodes

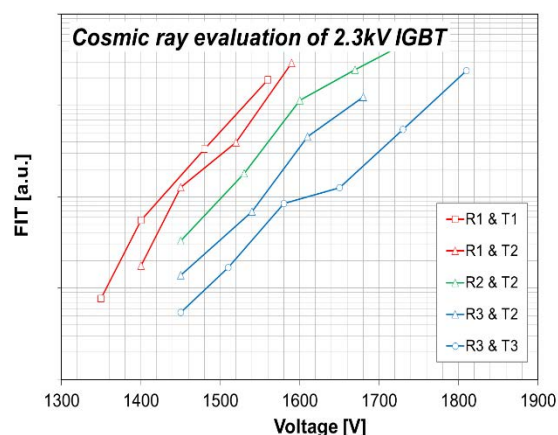


Fig. 1: Cosmic radiation failure rate of 2.3 kV IGBTs for different design parameters

and is shown in Fig. 2. Base material resistivity R and chip thickness T were varied. The numbers indicate increasing values.

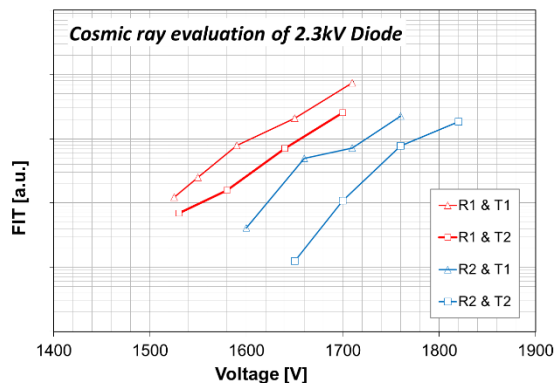


Fig. 2: Cosmic radiation failure rate of 2.3 kV diodes for different design parameters

A vertical design suitable for DC-link voltages up to 1500 V was chosen for further development.

Evaluating the design variations with respect to the blocking capability and the dynamic overvoltage during a switching event at a given FIT rate leads to a nominal blocking voltage of 2.3 kV.

The specific requirements of the targeted application are taken into account in the further development of the devices. In solar central converters, switching frequencies of up to 3.5 kHz are used and there is no limitation of the voltage and current slopes during switching. Thus, fast switching devices are targeted in the development; the controllability of the switching speed is not in focus. Since there are no strong requirements regarding cycling load capability and short-circuit robustness in the application, state-of-the-art aluminum (Al) chip metallization and Al bond wires as well as state-of-the-art solder joining technologies can be used.

With respect to short-term overload conditions in a grid failure like a low voltage ride through (LVRT), the solar central converter has to support and to stabilize the grid. Owing to these requirements, the technologies have been developed to allow permanent usage at $T_j=150^\circ\text{C}$ with short-term overload periods up to $T_{j\text{max}}=175^\circ\text{C}$.

3 IGBT technology

3.1 IGBT cell concept

To achieve the best performance, the most recent IGBT technology, TRENCHSTOP™ IGBT7, is used as the basis for the development. The cell

concept comprises parallel micro pattern trenches and narrow silicon mesas between the trenches, which provide strongly reduced static losses compared to the previous technology. The concept is described in [1] and [2].

The TRENCHSTOP™ IGBT7 allows for different contact schemes in order to tailor the device performance according to application requirements. A schematic of the cell concept, already presented in [1], is shown in Fig. 3. A scheme which connects more of the Si mesas to the emitter potential was selected for the 2.3 kV IGBT. This leads to a higher hole current during turn-off, and thus to faster switching. Additionally, a lower gate charge has been achieved by the adapted contact scheme.

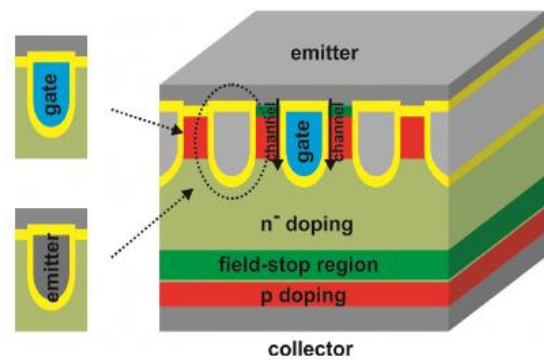


Fig. 3: Schematic of the IGBT micro pattern trench cell design, taken from [1]

The commutation behavior of the diode is influenced by the contact scheme as well. Different contact schemes were compared with respect to their influence on the diode. Figure 4 shows the transient switching of a 2.3 kV diode combined with two different IGBT versions, named C2 and C3. The voltage transient of the diode is plotted for different gate resistances R_G used for the IGBT in the five columns. When the diode is combined with the IGBT C3, the oscillations are clearly reduced even at low R_G .

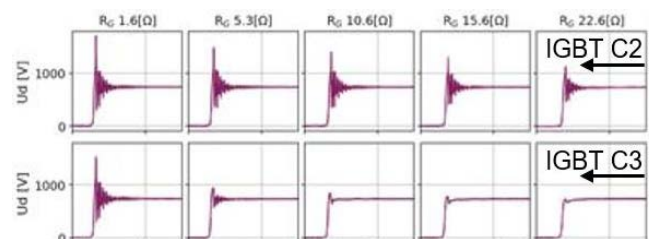


Fig. 4: Transient diode switching with two different IGBT variants for different R_G

The resulting total losses of the switching event are plotted in Fig. 5 with the overvoltage of the diode as parameter for its softness. This picture shows that the selected IGBT contact scheme allows for a better trade-off between diode softness and total losses.

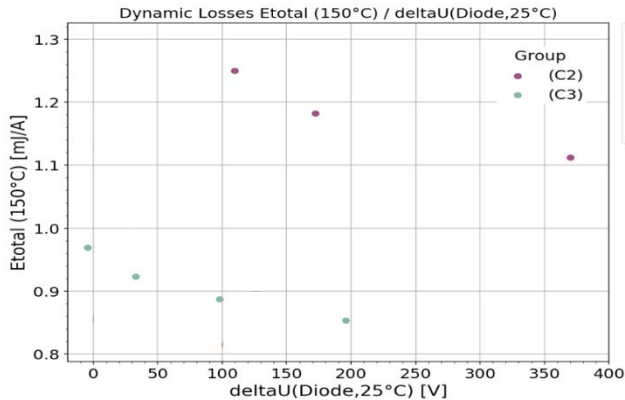


Fig. 5: Total switching losses as a function of diode overvoltage ΔU for two different IGBTs

To allow the device to be used in a NPC2 topology with a 1200 V common collector module, the device has also been developed with respect to switching performance when combined with a 1200 V emitter-controlled 7th generation (EC7) high-power diode.

3.2 Electrical performance of IGBT

The performance of IGBTs is usually given in terms of trade-offs, such as the well-known trade-off between static and dynamic losses and further restrictions with respect to customer requirements. The following plots give an overview of possible choices for the IGBT performance. The optimization is limited by the thickness, which was defined as described in Section 2 and Fig. 1 for the cosmic radiation robustness, and the contact scheme which has been chosen in Section 3.1 with respect to diode softness.

Figure 6 shows the turn-off losses E_{off} as a function of the conducting losses, represented by the saturation voltage V_{CEsat} , for the two temperatures 25°C and 150°C. Conditions for the investigated 2-level switching are $V_{DC}=1200$ V, and nominal conditions regarding current density. The remaining fine-tuning focuses on the turn-off losses. According to the essentials of solar applications, the turn-off behavior of the IGBT is tailored to be in the so-called self-controlled regime, and thus not controllable by an external R_G .

A wide range of V_{CEsat} and E_{off} can be addressed by varying the p-doped emitter of the device.

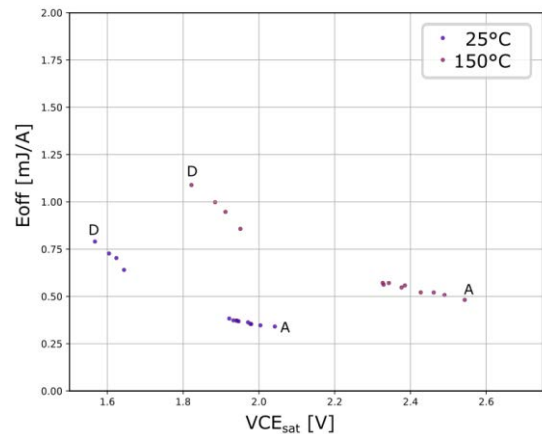


Fig. 6: IGBT turn-off losses E_{off} as function of saturation voltage V_{CEsat} at 25°C and 150°C

The turn-on losses are much less sensitive to a variation of the p-emitter. The resulting losses for $T=25^\circ\text{C}$ and $T=150^\circ\text{C}$ are shown in Fig. 7.

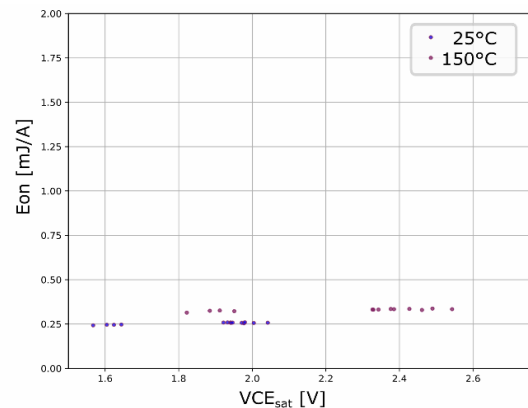


Fig. 7: IGBT turn-on losses E_{on} as a function of conducting losses V_{CEsat} at 25°C and 150°C

The turn-on losses can instead be influenced by adjusting the turn-on resistance R_{Gon} and thus, the switching speed di/dt . The reduction of the R_{Gon} is

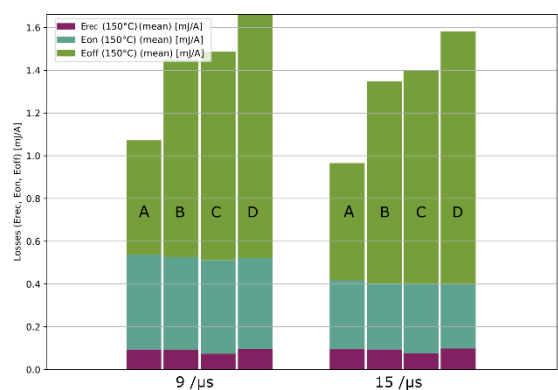


Fig. 8: Summary of total losses, E_{off} (green), E_{on} (blue) and E_{rec} (magenta) for two switching speeds and four vertical optimizations (A-D)

limited by the softness and the commutation robustness of the diode. Figure 8 shows the total switching losses for two different switching speeds.

The di/dt is normalized to the nominal current of the device. ($di/I_{NOM}/dt$). With higher di/dt , the turn-on losses of the IGBT are reduced while turn-off losses and E_{rec} are nearly unchanged.

Due to the optimization for 2-level solar inverter operation with $\cos(\phi) > 0$, recovery losses can almost be neglected.

4 Diode technology

4.1 Diode concept

The development of the 2.3 kV diode technology is strongly interlinked with the development of the 2.3 kV IGBT to ensure an optimum interaction of both devices in the application. The technology is based on the emitter-controlled 7th generation technology, which is tailored to the specific requirements of solar central converters.

The diode is optimized with respect to a reduced reverse recovery charge Q_{rr} , which in turn leads to low turn-on losses E_{on} of the IGBT.

The vertical design is mainly defined by the requirements concerning the cosmic radiation robustness at DC-link voltages up to 1500 V as described in Section 2 with the resulting failure rate shown in Fig. 2. For further parameters of the vertical structure, the same methods used for the 5th generation diode, as described in [3], were applied, which ensure a soft switching behavior despite the low Q_{rr} . Figure 9 compares the relative

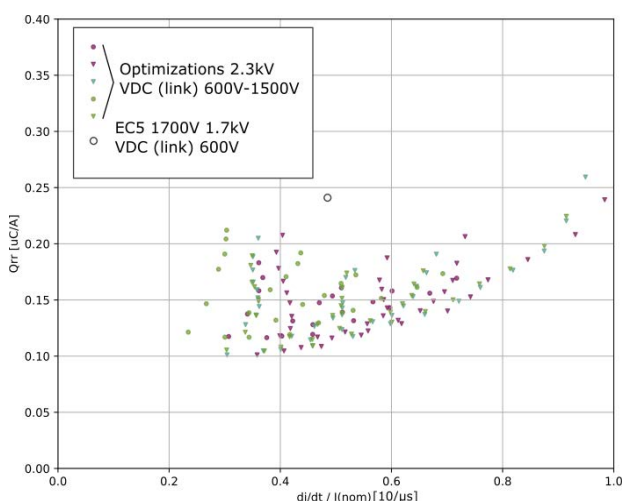


Fig. 9: Normalized recovery charge of the EC7 2.3 kV compared to EC5 1.7 kV and EC5 1.7 kV at relative switching speed

recovery charge (with respect to the current level of the switching event) and the relative switching speed di/dt (with respect to current class I_{NOM}) of the previous EC5 1700 V and the presented device. Even in a wide range of possible DC-link voltages from 600 V to 1500 V, the Q_{rr} remains lower than the EC5 1700 V.

4.2 Electrical performance of diode

The emitter controlled diode concept offers two major levers for adjusting the performance: emitter efficiency of both the cathode and anode side and the charge carrier lifetime adjustment. Figure 10 covers the diode's influence on the turn-on loss. This, in turn, is a direct result of the above-mentioned low recovery charge Q_{rr} as shown in Fig. 9.

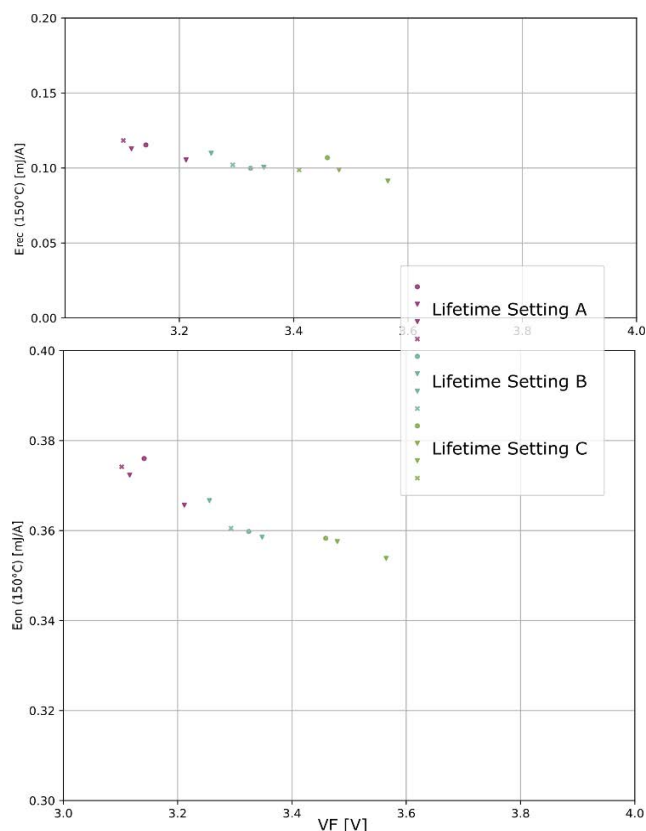


Fig. 10: Normalized turn-on and recovery loss for different lifetime adjustments and emitter adjustments on EC7 2.3 kV

The trade-off in VF (diode forward voltage drop) versus diode-caused dynamic losses is rather slight compared to the previous EC5 1700 V. The contribution of the higher VF compared to EC5 1700 V to the overall losses of solar inverters is negligible.

5 Switching in PrimePACK™ 3+ half-bridge module

A variant of the 2.3 kV IGBT and a variant of the 2.3 kV diode were chosen and built in a PrimePACK™ 3+ module in standard half-bridge configuration. The switching performance was evaluated in the standard 2-level configuration.

Figures 11 and 12 show the turn-off waveforms of the IGBT for an applied DC-link voltage of $V_{DC}=1500$ V at a current of $I=1800$ A and the two temperatures $T=25^{\circ}\text{C}$ and $T=150^{\circ}\text{C}$, respectively. An external R_{Goff} of 3.3 Ohm was chosen to guarantee oscillation-free switching.

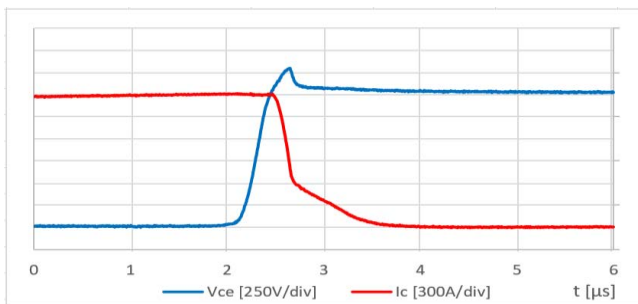


Fig. 11: Turn-off waveform of IGBT, $V_{DC}=1500$ V, $I_C=1800$ A, $R_{Goff}=3,3$ Ohm, $T_{vj}=25^{\circ}\text{C}$

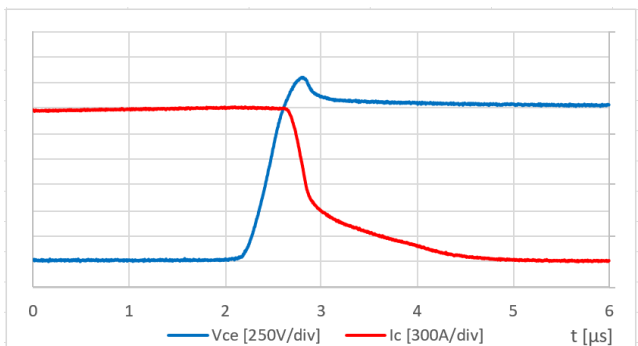


Fig. 12: Turn-off waveform of IGBT $V_{DC}=1500$ V, $I_C=1800$ A, $R_{Goff}=3,3$ Ohm, $T_{vj}=150^{\circ}\text{C}$

The resulting waveforms show very soft turn-off behavior and only small overvoltage under these conditions.

The turn-on waveforms at $T=25^{\circ}\text{C}$ and $T=150^{\circ}\text{C}$ are shown in Fig. 13 and Fig. 14, respectively.

For the turn-on, another R_G was chosen and set to $R_{Gon}=0.82$ Ohm. DC-link voltage and current level are identical to the switching-off event.

The waveforms are very smooth again, which indicates that the device can be used up to this current level without any problem.

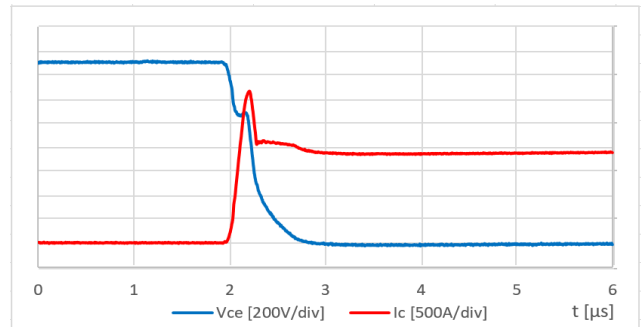


Fig. 13: Turn-on waveform of IGBT, $V_{DC}=1500$ V, $I_C=1800$ A, $R_{Gon}=0,82$ Ohm, $T_{vj}=25^{\circ}\text{C}$

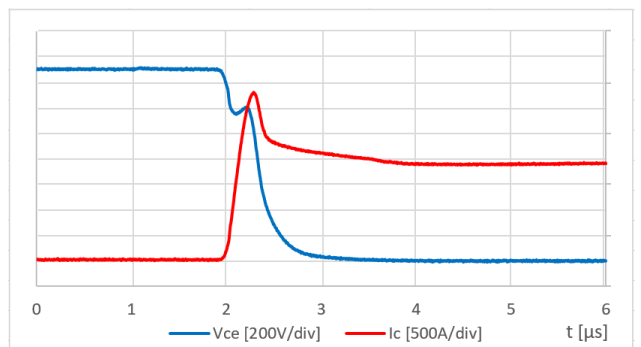


Fig. 14: Turn-on waveform of IGBT, $V_{DC}=1500$ V, $I_C=1800$ A, $R_{Gon}=0,82$ Ohm, $T_{vj}=150^{\circ}\text{C}$

Finally, the switching behavior of the 2.3 kV diode has been analyzed as well. Again the waveforms are shown for the temperatures $T=25^{\circ}\text{C}$ and $T=150^{\circ}\text{C}$ in Figures 15 and 16 respectively.

Similar to the IGBT, the diode shows oscillation-free switching at the presented conditions.

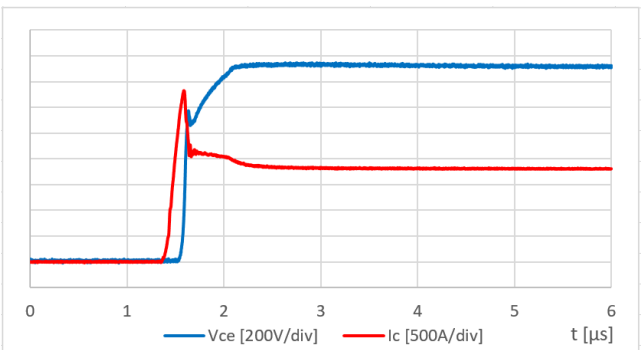


Fig. 15: Diode-recovery waveform, $V_{DC}=1500$ V, $I_C=1800$ A, $R_{Gon}=0.82$ Ohm, $T_{vj}=25^{\circ}\text{C}$

Under the conditions with high DC voltage $V_{DC}=1500$ V, nominal current $I_{Cnom}=1800$ A and low junction temperature $T_{vj}=25^{\circ}\text{C}$ (see Fig. 11), the switching speed (di/dt) at turn-off is moderate. In combination with the low-inductive DC-link design and the low-inductive PrimePACK™ 3+ module, this moderate di/dt results in a limited

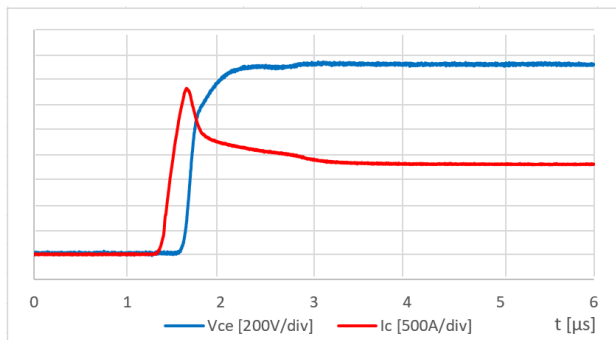


Fig. 16: Diode-recovery waveform, $V_{DC}=1500\text{ V}$, $I_C=1800\text{ A}$, $R_{Gon}=0.82\text{ Ohm}$, $T_{vj}=150^\circ\text{C}$

overvoltage shoot $\Delta V_{CE} = -L \cdot di/dt$ and a maximum voltage of $V_{CEmax} < 1850\text{ V}$. This value is well below the rated maximum voltage of $V_{NOM}=2.3\text{ kV}$ of the modules without the need for any external active V_{CE} clamping. These excellent results allow the operation of this power module without overvoltage shoot limitation during regular operation conditions. The significant advantage of this is a reduction in the number of components, and is a further step towards a simplified inverter design.

6 Output power

The 2.3 kV IGBT7 and EC7 technologies have been optimized with a clear focus on MW-range solar central inverters with a DC-link voltage of $V_{DC}=1500\text{ V}$. Implementing the new chipset in the PrimePACK™ 3+ housing, a new power module in half-bridge configuration with nominal current of 1800 A is feasible: the FF1800R23IE7.

Care has been taken to define a trade-off point that would suit applications based on both 2-level as well as 3-level NPC2 topologies. The latter has been evaluated considering the 2.3 kV PrimePACK™ half-bridge module in combination with the new 1200 V PrimePACK™ in common collector configuration [4].

The power output for both configurations has been evaluated by means of application simulation under the following conditions: $T_a=60^\circ\text{C}$, forced-air cooled heat sink, $f_{sw}=3.3\text{ kHz}$, $V_{DC}=1200\text{ V}$, $PF=1$. The thermal limits for the semiconductors are set to $T_{vj,op}=T_{vj,op,max}=150^\circ\text{C}$. Previous technologies required system developers to allow for some buffer between the operating temperature of the power module ($T_{vj,op}$) and the maximum rated operating temperature ($T_{vj,op,max}$) to account for overload conditions and failure modes such as low voltage ride-through (LVRT). The 2.3 kV chipset is specified to withstand junction temperatures (T_{vj}) up to 175°C for short time periods, therefore a 25 K

temperature buffer for overload conditions and failure mode operation. Thanks to this extended temperature range, the operating temperature $T_{vj,op}$ can be kept close to the $T_{vj,op,max}$.

For 2-level inverters, two configurations have been considered: one with two modules per leg and one with three modules per leg in parallel.

For both configurations, a discontinuous pulse width modulation (DPWM) has been considered. Figure 17 shows the simulated output power for both configurations. The configuration with two modules per leg (2L-2M) delivers 800 kW per inverter, whereas the three-module configuration (2L-3M) delivers 1200 kW.

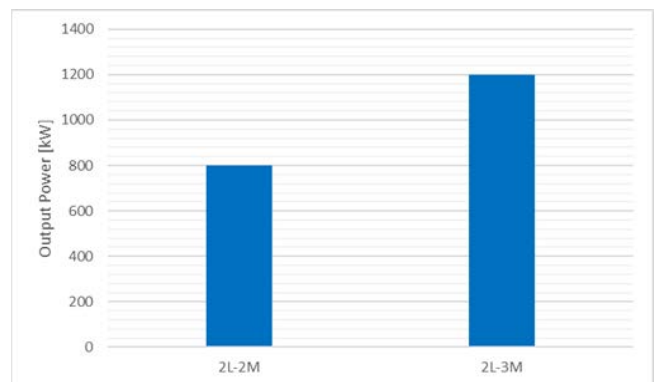


Fig.17: Simulated output power of a 2-level 3-phase inverter with two (2L-2M) and three (2L-3M) 2.3 kV half-bridge modules per leg

Two configurations have been considered for 3-level NPC2 as well: one with two modules per leg (3L-2M) and one with three modules per leg (3L-3M). The two-module solution includes a 2.3 kV PrimePACK™ in half-bridge configuration paired with a 1200 V PrimePACK™ in common collector configuration for the NPC path [4]. In the three-module solution, two PrimePACK™ 2.3 kV half-bridge modules are switched in parallel and paired with one 1200 V PrimePACK™ common collector. A schematic of the two 3-level setups is shown in Fig. 18.

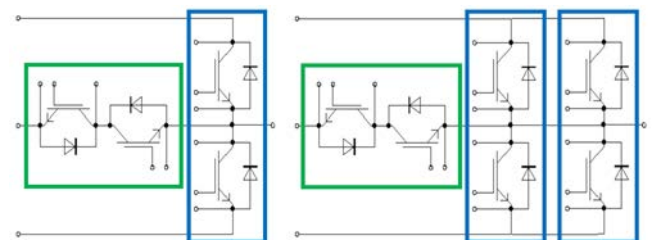


Fig. 18: 3 Level NPC2 topologies with PrimePACK™ left: two modules configuration; right: three modules configuration

Both configurations are simulated using the same conditions listed for the 2-level setup. Pulse modulation is done with a less complex space vector pulse width modulation (SVPWM). The simulated output power per inverter is shown in Fig. 19.

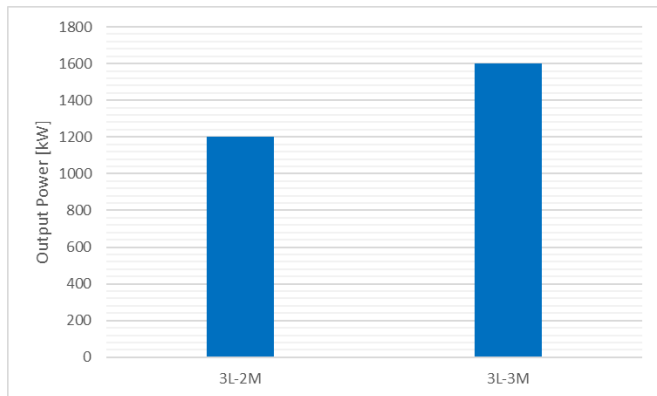


Fig. 19: Simulated output power of a 3-level 3-phase inverter with two (3L-2M) and three (3L-3M) modules per leg

The two-module configuration (3L-2M) delivers 1200 kW per inverter. By adding one additional module and implementing the three-module configuration (3L-3M), one can reach an output power of up to 1600 kW.

7 Summary

A chipset of an IGBT and a freewheeling diode of the new voltage class of 2.3 kV has been presented. The devices fulfill the specific requirements of solar central converters using a DC-link voltage of 1500 V. A low cosmic radiation failure rate at $V_{DC}=1500$ V is achieved. The performance enables operation of a PrimePACK™ 3+ module with a nominal current rating of 1800 A.

The design is well-suited for use in either a standard 2-level topology with only 2.3 kV half-bridge modules, or in a 3-level NPC2 topology in combination with a bidirectional switch at a nominal voltage of 1200 V. The performance in NPC2 topology is described in the paper “PrimePACK™ with 2.3 kV and 1200 V TRENCHSTOP™ IGBT7 enabling 1500 V-DC NPC2 in MW solar central inverter” also presented at this conference [4].

The devices are currently in development and electrical data presented in this paper are still subject to change.

8 References:

- [1] C. Jaeger et al: A new sub-micron trench cell concept in ultrathin wafer technology for next Generation 1200 V IGBTs“, Proc. ISPSD, pp. 69-72, 2017.
- [2] F. Wolter, W. Rösner, M. Cotorogea, T. Geinzer, M. Seider-Schmidt, K.-H. Wang, “Multi-dimensional trade-off considerations of the 750 V Micro Pattern Trench IGBT for Electric Drive Train Applications“, Proc. ISPSD, pp. 69-72, 2017
- [3] Santos et al: “Novel Emitter Controlled Diode with copper metallization in ultrathin wafer technology: setting a performance benchmark“, Proc. ISPSD 2017, pp 121-122, Sapporo, Japan
- [4] J. Esch, S. Mansueto, W. Rusche, K. Yilmaz, S. Thangavel, “PrimePACK™ with 2300 V and 1200 V TRENCHSTOP™ IGBT7 enabling 1500 V-DC NPC2 in MW solar central inverter“, PCIM 2020, Nuremberg, Germany